Accuracy tests

1. Cylindrical geometry

Transport equation for the temperature has been solved for constant source and diffusivity distributions. All convective fluxes were neglected. At this first step, the cylindrical plasma was considered and the equilibrium equation has been ignored. The central temperature T_0 was selected as a characteristic of the numerical properties.

A series of runs varying number of the radial grid nodes $N_\rho = 455, 201, 101, 51, 21, 11$ and time step $\tau[\mathrm{s}] = 10^{-5}, 10^{-4}, 10^{-3}, 10^{-2}, 10^{-1}, 10^{0}$ has been performed. The case $N_\rho = 455$, $\tau = 10^{-5}$ s was selected as a reference for assessment of the others. Deviations of all the runs

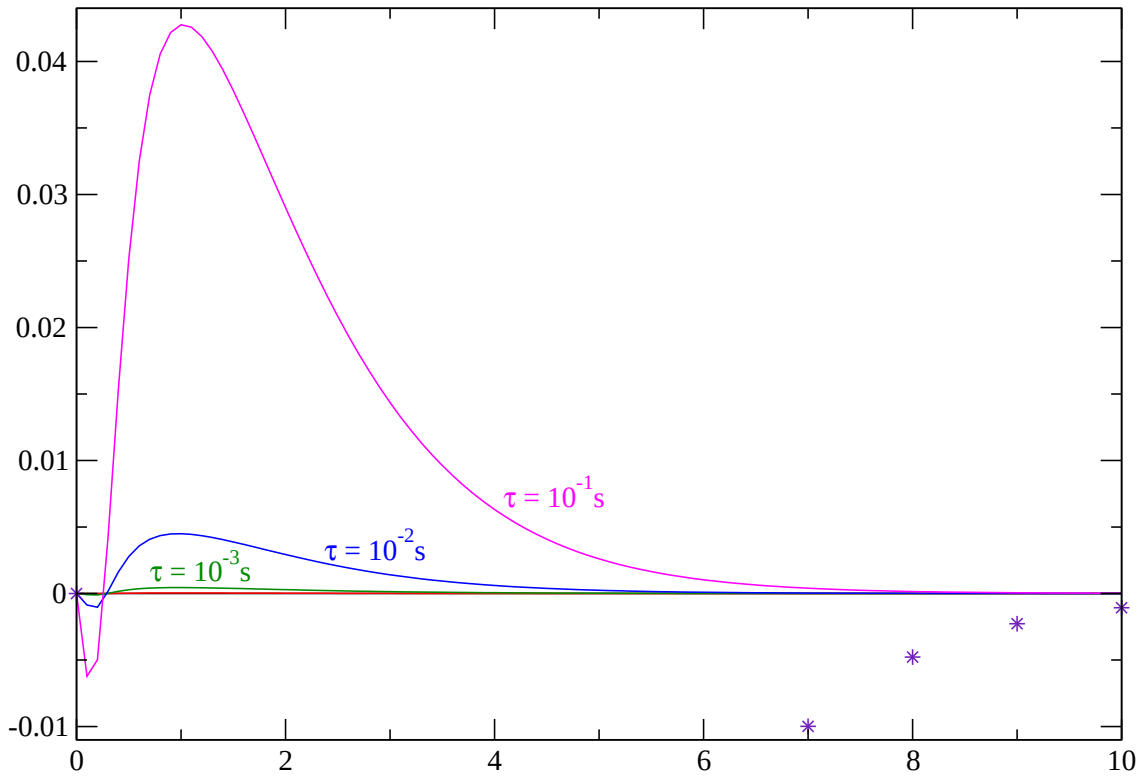

Fig. 1. Deviation of different runs from the reference run is shown for different values of the time step τ and ρ-grid size $N_\rho = 455$.

from the reference one are shown in Fig. 1. It is seen that the maximum errors are achieved at $t \approx 1$ s for all values of τ and then decay to zero at steady state. Even the time step of $\tau = 1$

s (shown in Fig. 1 with stars) converges to the steady state quite well although showing a huge delay in the evolution. As one could expect the error behaves as $\mathcal{O}(\tau)$ decaying by an order of magnitude with each step in τ. This is illustrated by the next Fig. 2 where the same graphs are shown in logarithmic scale. Figs. 1 and 2 show the absolute errors of different solutions. The relative error is approximately by a factor of 2 smaller because $T_0(t)$ varies from 1.45 till 3.87. Unevenness of the curves below 10^{-5} is caused by a reduced accuracy of the data stored for the plots (7 decimal digits). Having in mind that the characteristic time for these runs (energy confinement time τ_E) is approximately 0.8 s we outline the properties of τ-convergence:
1) At $\tau/\tau_E \leq 0.05$ the time evolution is described within the accuracy of 1%.
2) The maximum deviation appears at $t \approx \tau_E$ independently of the time step.
3) Steady state (if achieved) can be reasonably described even at $\tau > \tau_E$.

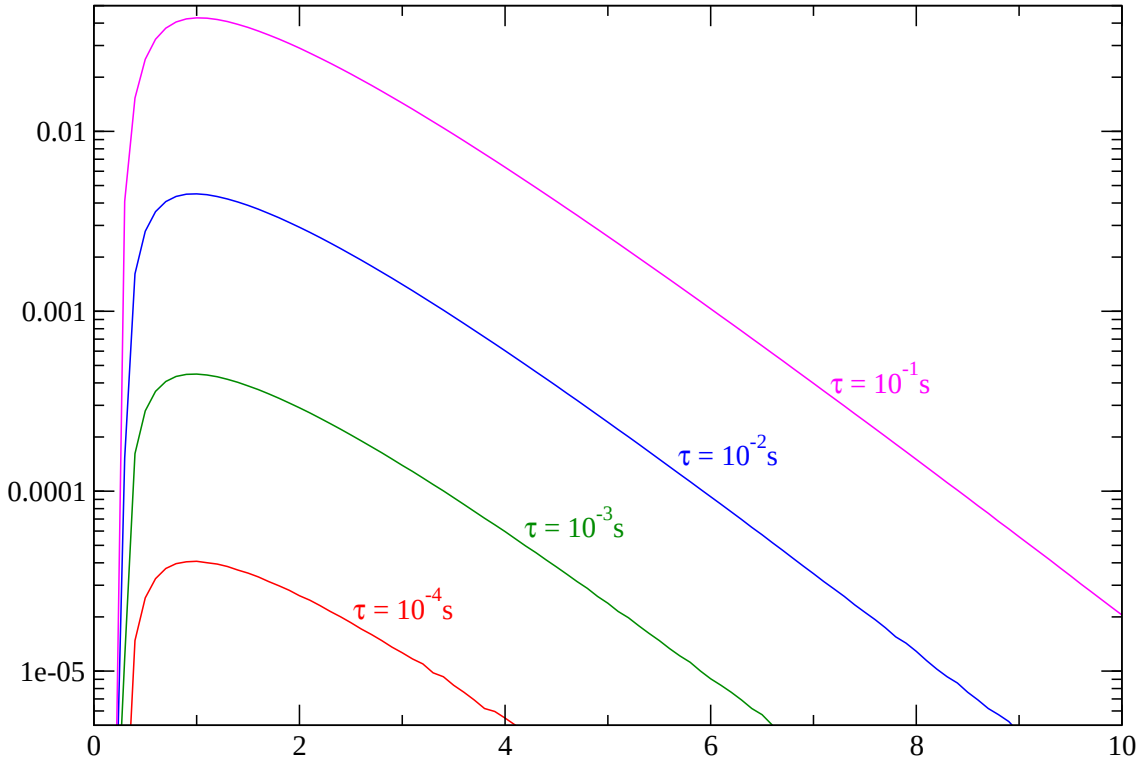

Fig. 2. The same as in Fig. 1 in logarithmic scale.

As a general remark, we observe that the realistic transport modelling imposes more severe limitations than those derived from this simplified study. In particular, a non-linearity of the problem results in instability of the numerical solution that appears in spite of fully implicit (backward Euler) in the second order derivative T'' numerical scheme. The requirement of the numerical stability keeps the time step far below the values forced by the requirement of the reasonable numerical accuracy.

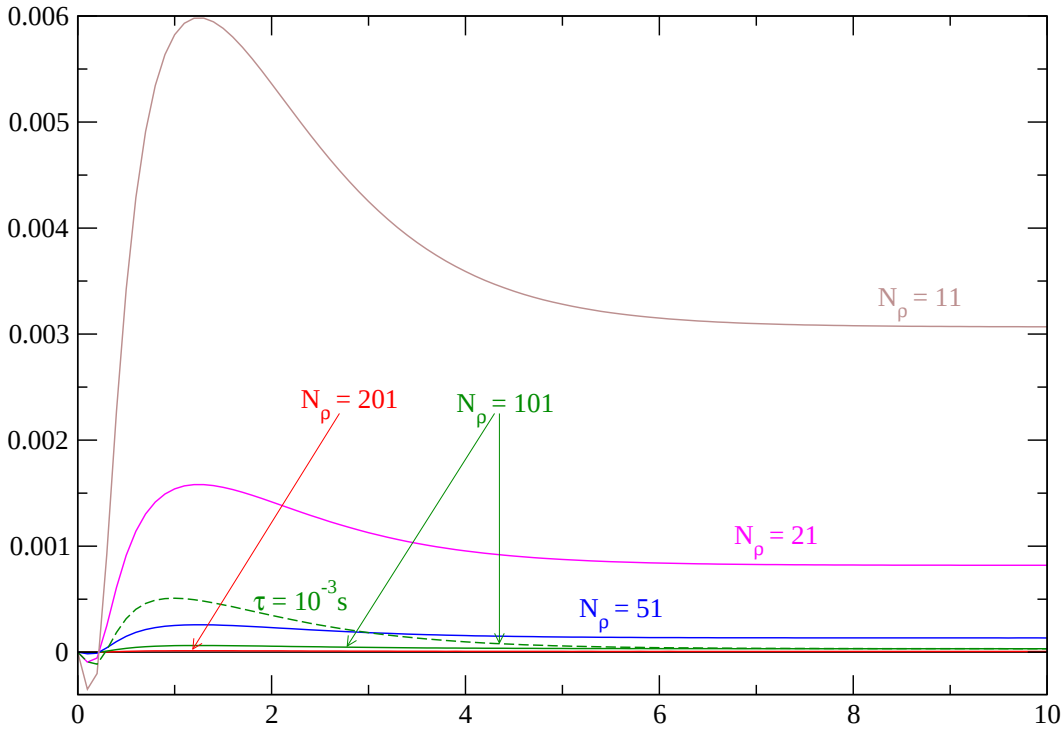

Fig. 3. Deviation of different runs from the reference run is shown for different size of the ρ-grid and $\tau = 10^{-5}$ s (solid lines) and $\tau = 10^{-3}$ s (dashed line).

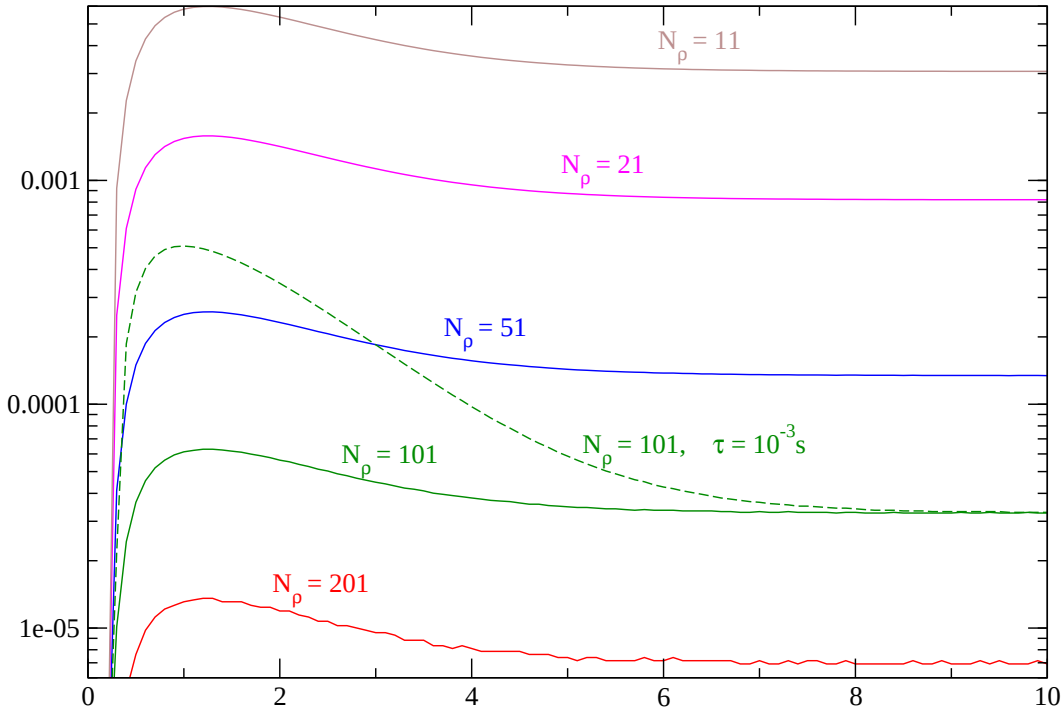

Fig. 4. The same as in Fig. 3 in logarithmic scale.

The next series of curves in Figs. 3 and 4 shows a dependence of the numerical error on the space grid size in linear and logarithmic scales, respectively. One sees that even at 11 grid nodes the error does not exceed 0.5%. In practice it means that except for some specific cases (ITB, sawteeth, tearings) a grid of 20 cells, i.e. 21 grid points, (the number has been fixed in TRANSP for a decade) delivers an accuracy sufficient for most tokamak applications. Further examination shows that the error behaves as $\mathcal{O}(N^{-2})$ in accordance with the general theory. Another observation is that, unlike the τ-dependence, the saturated value of T_0 is different for each grid size. Nevertheless, this difference is small and cannot be considered as meaningful.

In order evaluate the relative influence of the grid-node number and of the time step we put on the same plot also one curve with a larger time step. It is seen that from the point of accuracy duplication of a number of grid points is more efficient than decrease of the time step. The time consumption increases approximately linearly with both, the number of time steps and the number of grid points although the latter is valid for a simple transport problem only.

2. Toroidal geometry

All runs of the previous section have been repeated for the toroidal geometry where the plasma equilibrium was calculated by a 3-moment equilibrium solver EMEQ. EMEQ has been used at the radial grid of $N_{eq} = \min(101, N_\rho)$ nodes. Fig. 4 shows the same dependences as Fig. 2 for a tokamak with a circular cross-section ($R_0 = 6.2$ m, $a = 2$ m, $B_0 = 5.3$ T, $I_{pl} = 6$ MA). Comparison shows that adding of the equilibrium constraints does not affect the accuracy of the calculations noticeably. Qualitative behaviour also does not change with one exception: As clearly seen from Fig. 5 a new slow time scale appears in the problem. This is the skin time that comes into the problem because the equilibrium equation couples together the current diffusion and the energy/particle balance equations. In this particular case, the skin time is about 10 s. It exceeds the energy confinement time more than by a factor of 10 so that one needs to wait for about 30–40 s before a good steady state is achieved.

Nevertheless, we conclude that neither the influence of the tokamak geometry nor the slow equilibrium drifting changes the main outcome of this exercise:

The choice of $N_\rho = 101$ and $\tau = 0.001$ s gives a reasonable time/space step combination that allows to keep the relative error below the limit of 0.5‰ (5×10^{-4}). This combination is proposed for ETS V&V study.

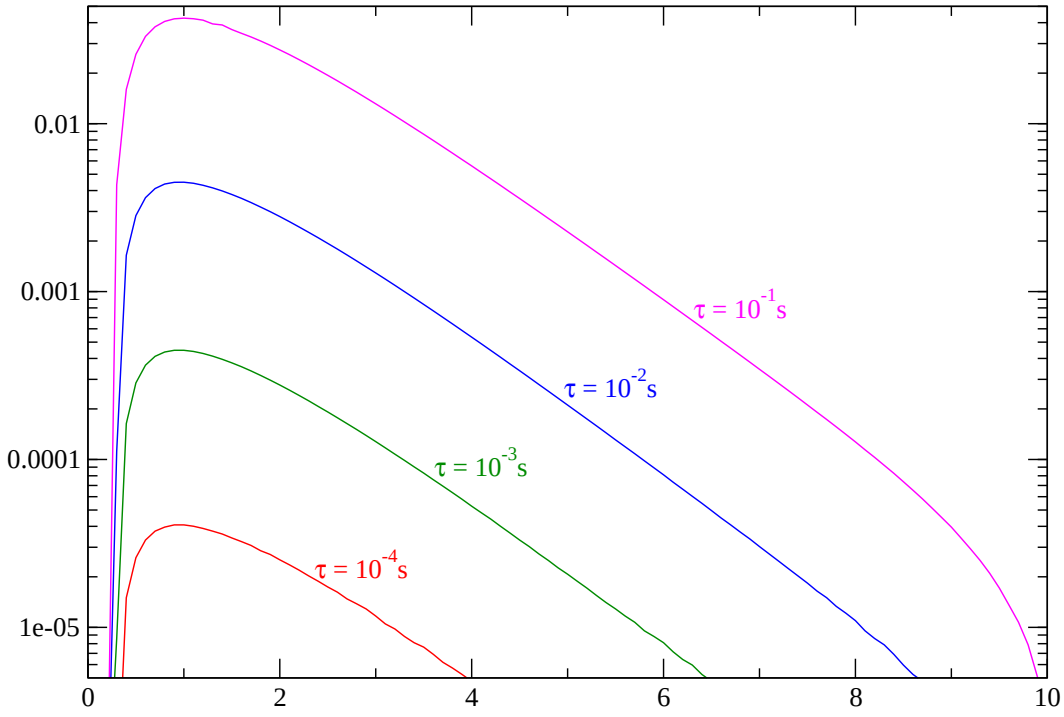

Fig. 4. The same as in Fig. 2 with the equilibrium switched on.

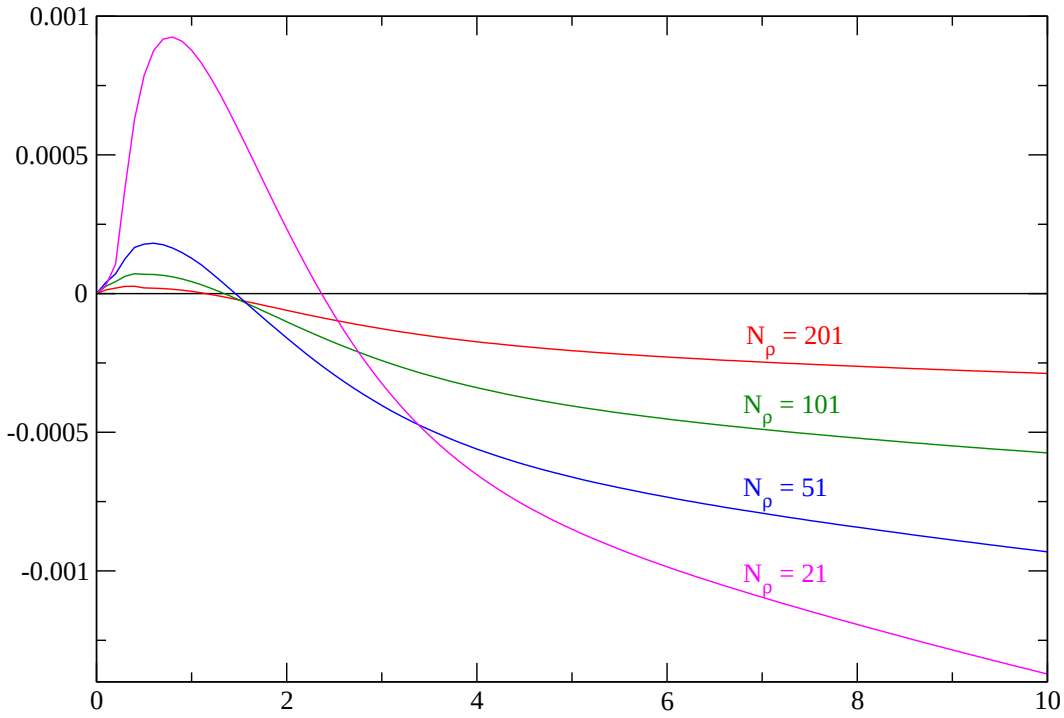

Fig. 5. The same as in Fig. 3 with the equilibrium switched on.